

Hydrological hazard mapping in Rupandehi district, west Nepal

Megh Raj Dhital¹, Rajendra Shrestha², Motilal Ghimire³,
Ghan Bahadur Shrestha⁴, and Dhruba Tripathi⁴

¹Central Department of Geology, Tribhuvan University, Kathmandu, Nepal

²Butwal Power Company Pvt. Ltd, Nepal

³Central Department of Geography, Tribhuvan University, Kathmandu, Nepal

⁴Mountain Risk Engineering Unit, Tribhuvan University, Kathmandu, Nepal

ABSTRACT

Large-scale (1:25,000) integrated hydrological hazard mapping was carried out in the Rupandehi district of west Nepal. The main hazard types in the study area were landslides, debris flows, floods, bank undercutting, and inundation. The maps were prepared on the basis of field observation of damages and hazards as well as using available topographic maps, digital data, satellite imageries, and aerial photographs. The information gathered was digitised and analysed using mainly ArcView and ILWIS GIS systems and HEC-RAS.

INTRODUCTION

In Nepal, hydrological disasters cause a huge loss of lives and property annually. As a first step towards mitigating or controlling such problems, it is necessary to prepare hydrological hazard maps. Consequently, the Department of Water-Induced Disaster Prevention has initiated a programme of large-scale (1:25,000) hazard mapping in some districts of Nepal. The paper summarises the outcomes of a pilot study of such efforts in the Rupandehi district of west Nepal.

The Rupandehi district (Fig. 1) lies in the Western Development Region of Nepal and its headquarters are at Bhairahawa (Siddhartha Nagar). It suffers from various types of hydrological hazards (Table 1). The study area covers about 1011.3 sq km and is accessible by roads, trails, and highways. The road network is well developed in the Terai (Table 2).

PREVIOUS STUDIES

Brunsdan et al. (1975) were one of the first to develop a geomorphological map of a road corridor in Nepal. Based on their findings, the Leoti Khola–Mulghat sector of the Dharan–Dhankuta road alignment was relocated.

Kojan (1978) studied the landslide problems along the Godavari–Dandeldhura road. He identified the main hazardous areas along the road sector and recommended various methods of slope stabilisation. He also concluded that about 26% increase in landslide was due to human activities.

Wagner (1981) was probably the first to prepare a landslide and gully erosion hazard map based on field observations. For this purpose, he prepared various maps depicting rock and soil type, slope angle, aspect, and orientation of discontinuities along the Siddhartha Highway around Waling in west Nepal. Deoja et al. (1991) further

developed this method and proposed various ratings for attributes such as rock type, soil type, slope angle, relative relief, groundwater, surface hydrology, folds, and faults.

Probably, the first detailed landslide hazard mapping was carried out along the Tulsipur–Sallyan, Ghorahi–Piuthan, and Piuthan–Libang roads of mid west Nepal (DoR/USAID 1986). These maps were derived from engineering geological mapping of the road alignment on a scale of 1:5000, aerial photo interpretation, and kinematic analysis of joints.

Feasibility- and detailed-stage landslide hazard mapping was carried out along the Baitadi–Darchula road alignment in far west Nepal (Dhital et al. 1991). The hazard mapping was based on the preparation of engineering geological maps, slope maps, soil type and soil depth maps, and the maps depicting the relationship between discontinuities and slope aspect. The hazard maps of feasibility stage showed overall hazard types whereas those of detailed stage depicted specific hazard types and their level.

DPTC (1996) carried out the detailed investigation, monitoring, and control of a landslide in the Ilam district of

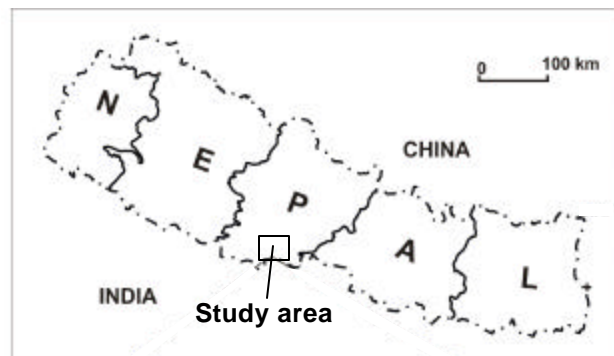


Fig. 1: Location map of the study area

Table 1: Summary of damage by floods and landslides from 1992 to 2002 in the Rupandehi district

| Disaster Date | Affected VDC (ward) | No. of deaths | No. of missing persons | No. of injured persons | No. of affected family | No. of livestock lost | No. of houses damaged | | | Land affected | Estimated loss (NRs) |
|---------------|---------------------|---------------|------------------------|------------------------|------------------------|-----------------------|-----------------------|--------|----------------|---------------|----------------------|
| | | | | | | | Completely | Partly | Shed destroyed | | |
| 1994 | | 1 | | 0 | 1 | 0 | 0 | 0 | | | |
| 1995 | | - | | - | - | - | - | - | - | - | - |
| 1997 | | - | | - | - | - | - | - | - | - | - |
| 1998 | | 18 | | 4 | 1448 | 1 | 128 | - | 1 | 0.14 ha | 68,190,300.00 |
| 1999 | | 4 | | 1 | 33 | 3 | 5 | 25 | 1 | | 390,500.00 |
| 2000 | | - | | - | - | - | - | - | - | - | - |
| 2-8-2001 | Kamhariya (4) | 1 | 1 | 2 | 1 | - | - | - | - | 8 Bigha | 4,500,000.00 |
| 30-7-2001 | Majahagobha (3) | | | | 1 | | 1 | | | | 9800.00 |

Source: Department of Narcotics Drugs Control and Natural Disaster Management, Government of Nepal. *One Kattha* = 1/20 of a *Bigha*, and one *Bigha* = 0.67772 ha

Table 2: Transportation network in the Rupandehi district

| Transportation | Length, km |
|----------------|-------------|
| Highway | 66 |
| Feeder road | 33 |
| District road | 250 |
| Other road | 60 |
| Cart tract | 204 |
| Footpath | 1695 |
| Runway | 4 |
| Total | 2312 |

east Nepal. The landslide is located on the left bank of the Mai Khola, at Km 62 of the Charali–Ilam road. The landslide came into existence during the road construction in 1984, and became quite hazardous during the road maintenance of 1992 and was further aggravated in the monsoon of 1995.

DPTC (1993) prepared a flood hazard map of the Bagmati River in the Sarlahi and Rautahat districts. HMG Nepal, UNDP, and ICIMOD (2001) carried out flood hazard mapping in two VDCs of the Chitwan and two VDCs of the Bardiya districts using geographic information system and remote sensing techniques coupled with field verifications.

HYDROLOGICAL ANALYSIS

The flood data of the Tinau River at the DHM station no. 390 (latitude: 27°42'10"; longitude: 83°27'50") were used for estimating different return periods. The flood data of other rivers and tributaries in the study area are not available. The annual maximum instantaneous flood discharge of the Tinau River for the period from 1964 to 1969 and from 1984 to 1992 is available from DHM (Table 3). Flood estimates for different return periods were made by applying the generalised extreme value I (EVI) and log Pearson Type III methods.

Table 4 shows the flood estimates in the Tinau River at the DHM station no. 390 for various return periods. The maximum value recorded at that station was adapted for

Table 3: Maximum instantaneous annual flood discharge data of the Tinau River at DHM Station No. 390

| Year | Discharge (m ³ /s) |
|------|-------------------------------|
| 1964 | 417 |
| 1965 | 2220 |
| 1966 | 1180 |
| 1967 | 1950 |
| 1968 | 2000 |
| 1969 | 600 |
| 1984 | 390 |
| 1985 | 325 |
| 1986 | 644 |
| 1987 | 580 |
| 1988 | 565 |
| 1989 | 457 |
| 1990 | 260 |
| 1991 | 288 |
| 1992 | 134 |

further analysis. The guideline recommended by WECS/DHM (1990) was used as a basis for estimating the flood flows in other rivers in the study area. Table 5 shows the prorated flood flows for various return periods in different tributaries.

Flood hazard mapping in the field

For the preparation of a hazard map, traverses were made along the Tinau, Dano, Rohini, and Kanchan river, and their tributaries. During the field study, detailed information regarding old river course, flood marks, bank height, bank cutting, channel shifting, and effect of flooding on civil structures, were collected. Local people were interviewed to get information on the history of river flooding, observed flood levels, socioeconomic impact of floods, and hazard assessment perception of the community.

Flood hazard mapping using numerical modelling

Since the field investigation showed considerable variation in the flood hazard zones from the desk study-stage flood hazard map, a new approach was necessary to apply. Field evidence as well as the interpretation of aerial

Table 4: Flood estimates for the Tinau River

| | | Method | | |
|---------------------------------|------------|-----------------|----------------------|---------|
| | | Generalised EVI | Log Pearson Type III | Adopted |
| Flood flows (m ³ /s) | 1 in 2-yr | 490 | 435 | 490 |
| | 1 in 5-yr | 905 | 778 | 905 |
| | 1 in 10-yr | 1180 | 1082 | 1180 |
| | 1 in 20-yr | 1440 | 1221 | 1440 |
| | 1 in 50-yr | 1786 | 2060 | 2060 |

Table 5: Flood estimates for tributaries

| Location | Flood flow, m ³ /s | | | |
|--|-------------------------------|------------|------------|------------|
| | 1 in 5-yr | 1 in 10-yr | 1 in 20-yr | 1 in 50-yr |
| Confluence of the Suili Khola and Dano River | 42 | 56 | 72 | 118 |
| Confluence of the Baurba Khola and Dano River | 64 | 85 | 109 | 173 |
| Inguriya River | 202 | 266 | 334 | 503 |
| Confluence of the Kanchan River and Dano River | 239 | 316 | 395 | 589 |
| Tributary from the village Dhamasar | 58 | 78 | 99 | 159 |

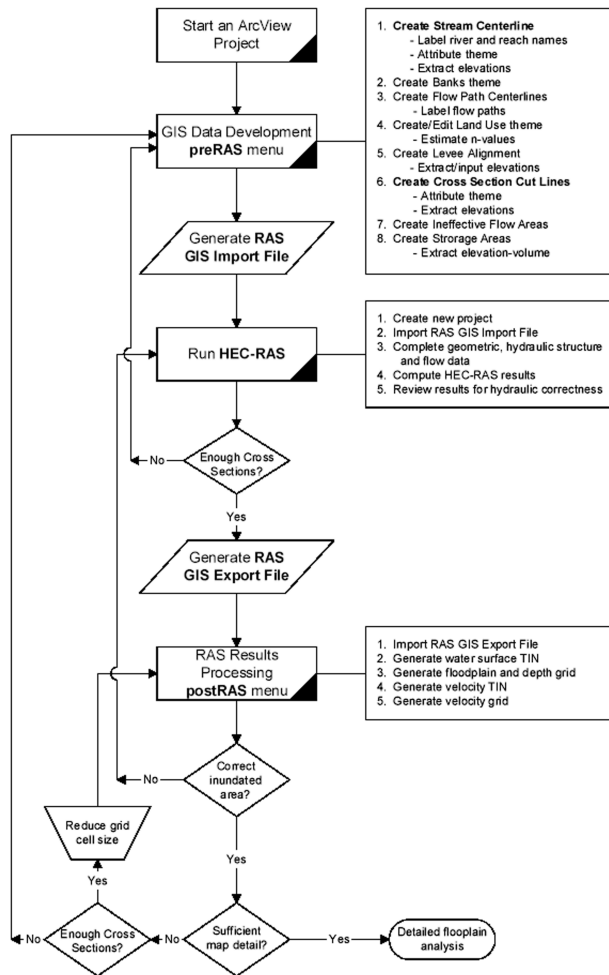


Fig. 2: Process flow diagram for using HEC-GeoRAS

photographs, topographic maps, and satellite imageries indicated that a reliable estimation of floodwater distribution in the surrounding areas is required for preparing a flood hazard map. The evaluation of hydrological, hydraulic, topographic, and social parameters were also required for this purpose. Hence, the final flood hazard map was prepared using HEC-RAS and ArcView GIS system. The floodplain analysis of the Tinau River and Dano River was carried out using one-dimensional numerical model HEC-RAS and ArcView GIS. HEC-GeoRAS extension for ArcView GIS was used as an interface between the two systems for the pre-processing and post-processing of the data in GIS.

During the pre-processing of the GIS data, a triangulated irregular network (TIN) was prepared from available contours and spot elevations. A series of line themes pertinent to developing geometrical data for HEC-RAS were created. The themes created are stream centre line, flow path centre line, main channel banks, and cross-sectional cut lines. An overview of the HEC-GeoRAS process is shown Fig. 2. After creating each RAS theme, GIS data (geometric data) were exported to run in HEC-RAS. The plan of the Tinau and Dano Rivers generated by ArcView GIS is shown in Fig. 3.

In the HEC-RAS, after importing the geometric data extracted from GIS, hydraulic data were entered. Flow data and associated boundary condition were also supplied. In the next step, water surface profile calculation for the flood of 5, 10, 20 and 50 year return periods were performed with a subcritical flow regime. Once the water surface profiles were calculated, the results were exported to GIS format.

At the last step, HEC-RAS results were imported into the GIS system and a floodplain map for each profile was developed. The longitudinal profiles of the two rivers are presented in Fig. 4 whereas a few typical cross-sections of the Tinau River are shown in Fig. 5 and 6, and a cross-section of the Dano River is given in Fig. 7. The plots of discharge versus water surface elevation at their respective locations are indicated in Fig. 8, 9, and 10. A flood hazard classification scheme based on this analysis is shown in Table 6, and flood hazard in the district is depicted in the integrated hydrological hazard map (Fig. 11).

HAZARD MAPPING

A landslide hazard map was prepared using the GIS based bivariate statistical technique developed by the International Institute of Aerospace Survey and Earth Sciences (ITC), the Netherlands. It is based on the quantitatively defined weight values. A weight value for a parameter class is defined as the natural logarithm of the landslide density in the class divided by the landslide density in the entire map. It is expressed as:

$$W_i = \ln(DenseClass / DenseMap) = \ln \frac{NPIX(S_i) / NPIX(N_i)}{\sum NPIX(S_i) / \sum NPIX(N_i)}$$

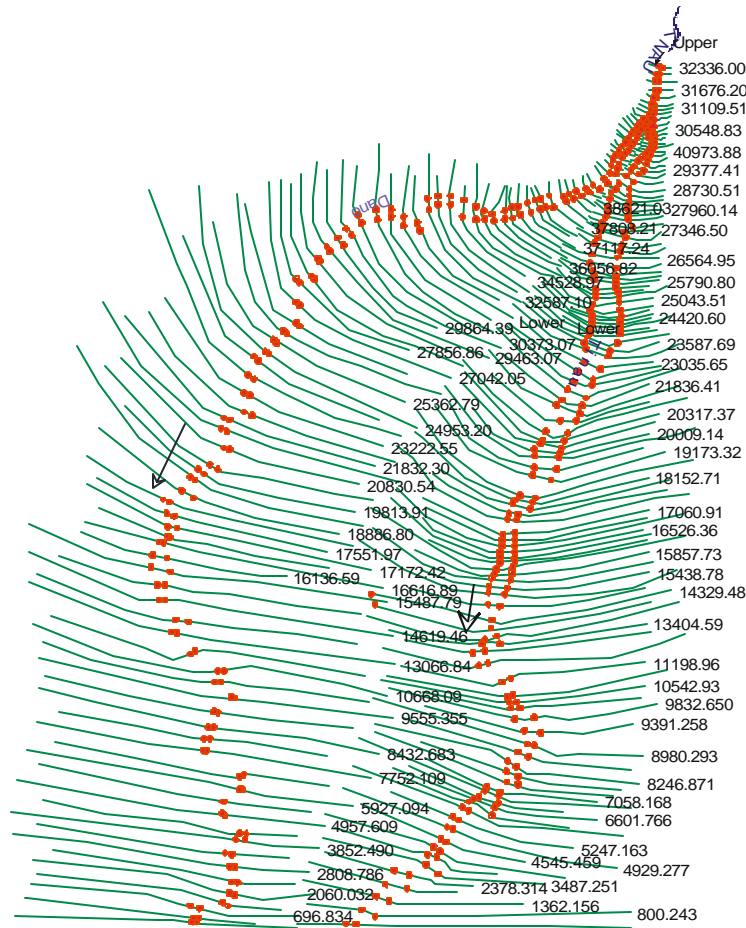


Fig. 3: Plan depicting river centre line, cross-section lines, and river stations of the Tinau and Dano Rivers

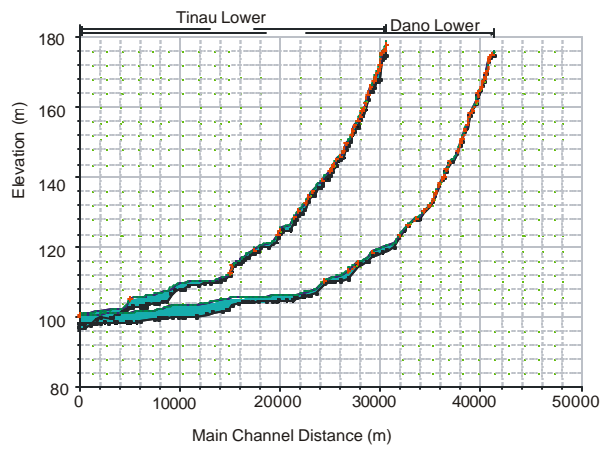


Fig. 4: Longitudinal profiles of the Tinau and Dano Rivers

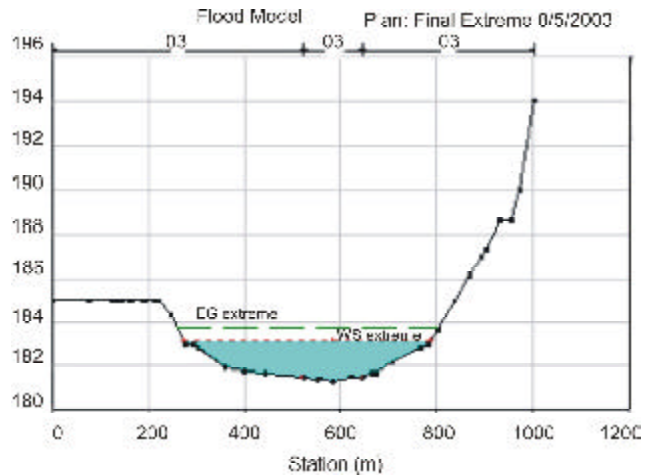


Fig. 5: Cross-section of the Tinau River (upper reach) at RS 31109.51

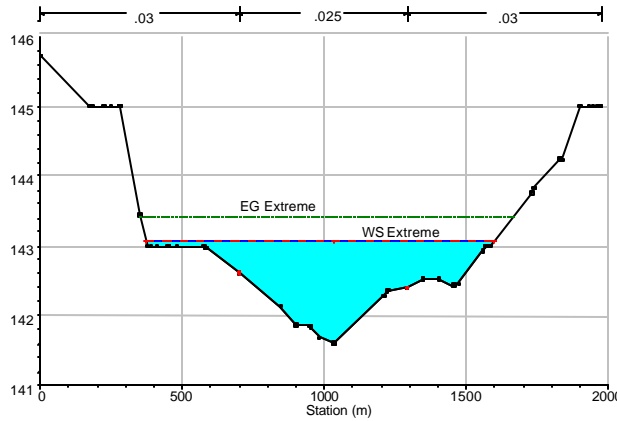


Fig. 6: Cross-section of the Tinau River (lower reach) at RS 25432.96

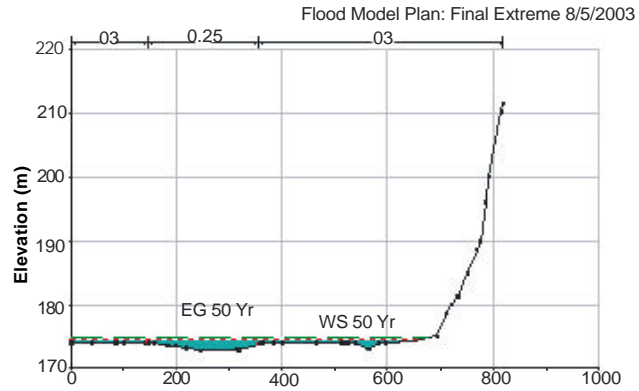


Fig. 7: Cross-section of the Dano River at RS 40973.88

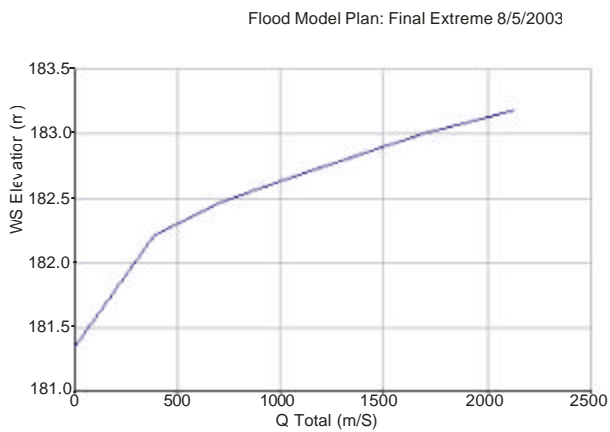


Fig. 8: Plot of discharge versus water surface elevation for the Tinau River (lower reach) at RS 31109.51

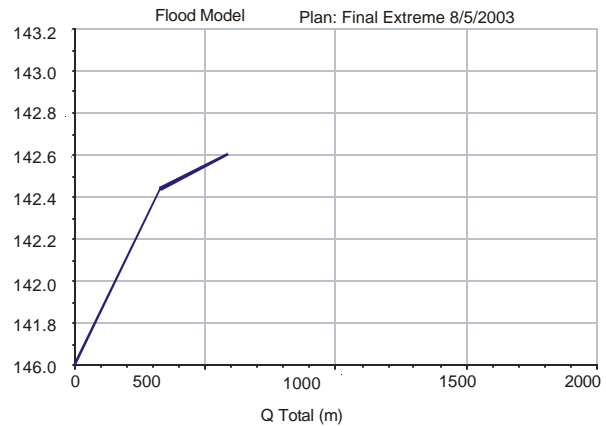


Fig. 9: Plot of discharge versus water surface elevation for the Tinau River (lower reach) at RS 25432.96

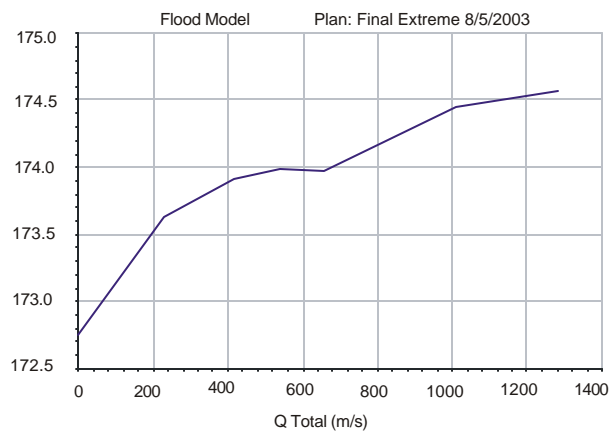


Fig. 10: Plot of discharge versus water surface elevation for the Dano River at RS 40973

where W_i = the weight given to a certain parameter class, $Dense\ Class$ = the landslide density within the parameter class, $Dense\ Map$ = the landslide density within the entire map, $NPIX(S_i)$ = number of pixels containing landslide in a

certain parameter class, and $NPIX(N_i)$ = total number of pixels in a certain parameter class.

To calculate the weights, a cross table (Table 7) was obtained by map crossing on ILWIS 2.1 GIS and Image Processing System developed by ITC. All input values for the formula were obtained from the cross table. The natural logarithm was used to give a negative weight when the landslide density was lower than the normal and a positive weight when it was higher than the normal.

The following maps were used to obtain the landslide and gully erosion hazard map:

- Weight map of slope gradient,
- Weight map of slope aspect,
- Weight map of land use and land cover,
- Weight map of fault distance,
- Weight map of relative relief,
- Weight map of geology,
- Weight map of slope shape, and
- Weight map of vegetation density.

Table 6: Flood hazard classification

| Hazard type | Depth of water (m) |
|-------------|--------------------|
| Very High | >1.6 |
| High | 0.8 – 1.6 |
| Moderate | 0 – 0.8 |
| Low | |

Table 7: Cross table of landslide hazard mapping attributes used in the bivariate analysis

| 1. Slope gradient | | | | | |
|----------------------|---------|-----------------|-------------------|-------------|----------|
| Slope (degrees) | Count | Landslide count | Landslide density | Coefficient | Weight |
| <15 | 1573694 | 4093 | 0.0026 | 0.0065 | -0.92 |
| 15-25 | 589365 | 4264 | 0.0072 | 0.0065 | 0.10 |
| 25-35 | 412262 | 5355 | 0.0130 | 0.0065 | 0.69 |
| 35-45 | 46619 | 862 | 0.0185 | 0.0065 | 1.05 |
| >45 | 41897 | 2456 | 0.0586 | 0.0065 | 2.20 |
| 2. Slope aspect | | | | | |
| Aspect | Count | Landslide count | Landslide density | Coefficient | Weight |
| Flat | 247285 | 239 | 0.0010 | 0.0065 | -1.87210 |
| North | 91240 | 89 | 0.0010 | 0.0065 | -1.87210 |
| Northeast | 44798 | 128 | 0.0029 | 0.0065 | -0.80699 |
| East | 962753 | 8034 | 0.0083 | 0.0065 | 0.24444 |
| Southeast | 130394 | 786 | 0.0060 | 0.0065 | -0.08002 |
| South | 154690 | 612 | 0.0040 | 0.0065 | -0.48548 |
| Southwest | 118231 | 768 | 0.0065 | 0.0065 | 0.00000 |
| West | 952062 | 6583 | 0.0069 | 0.0065 | 0.05968 |
| Northwest | 98 | 0 | 0.0001 | 0.0065 | -4.17339 |
| 3. Land use pattern | | | | | |
| Land use type | Count | Landslide count | Landslide density | Coefficient | Weight |
| Built-up area | 27785 | 0 | 0.0001 | 0.0065 | -4.17339 |
| Buildings | 8 | 0 | 0.0001 | 0.0065 | -4.17339 |
| Cutting | 6929 | 1248 | 0.1801 | 0.0065 | 3.32171 |
| Cultivation | 342846 | 135 | 0.0004 | 0.0065 | -2.78872 |
| Forest | 2162130 | 15239 | 0.0070 | 0.0065 | 0.07409 |
| Bush | 112524 | 564 | 0.0050 | 0.0065 | -0.26240 |
| Sand | 37323 | 50 | 0.0013 | 0.0065 | -1.60944 |
| Barren land | 5511 | 0 | 0.0001 | 0.0065 | -4.17339 |
| Riverbed | 5097 | 0 | 0.0001 | 0.0065 | -4.17339 |
| Pond or lake | 905 | 0 | 0.0001 | 0.0065 | -4.17339 |
| 4. Fault zone | | | | | |
| Distance above fault | Count | Landslide count | Landslide density | Coefficient | Weight |
| Within 200 m | 89872 | 100 | 0.0011 | 0.0065 | -1.77667 |
| Others | 2617396 | 17143 | 0.0065 | 0.0065 | 0.00000 |
| 5. Relative relief | | | | | |
| Relief class | Count | Landslide count | Landslide density | Coefficient | Weight |
| Flat (<1) | 448394 | 31 | 0.0001 | 0.0065 | -4.17339 |
| Low (1-20) | 1139348 | 2836 | 0.0025 | 0.0065 | -0.95555 |
| Medium (20-40) | 956107 | 8331 | 0.0087 | 0.0065 | 0.29155 |
| High (>40) | 121387 | 5855 | 0.0482 | 0.0065 | 2.00356 |
| 6. Geology | | | | | |
| Category | Count | Landslide count | Landslide density | Coefficient | Weight |
| Alluvial deposits | 598359 | 15 | 0.0001 | 0.0065 | -4.17339 |
| Middle Siwaliks | 829234 | 9009 | 0.0109 | 0.0065 | 0.51695 |
| Lower Siwaliks | 1274898 | 8219 | 0.0064 | 0.0065 | -0.01552 |
| 7. Slope shape | | | | | |
| Slope shape type | Count | Landslide count | Landslide density | Coefficient | Weight |
| Concave | 1048350 | 9989 | 0.0095 | 0.0065 | 0.37946 |
| Straight | 636877 | 324 | 0.0005 | 0.0065 | -2.56525 |
| Convex | 1016324 | 6926 | 0.0068 | 0.0065 | 0.04516 |
| 8. Vegetation | | | | | |
| Vegetation density | Count | Landslide count | Landslide density | Coefficient | Weight |
| Sparse | 421859 | 3041 | 0.0072 | 0.0065 | 0.10229 |
| Moderate | 640159 | 3679 | 0.0057 | 0.0065 | -0.13136 |
| Moderately dense | 230165 | 880 | 0.0038 | 0.0065 | -0.53683 |
| Dense | 1395684 | 8160 | 0.0058 | 0.0065 | -0.11395 |

Note: Coefficient = total landslide count/total count (which is about 0.0065)

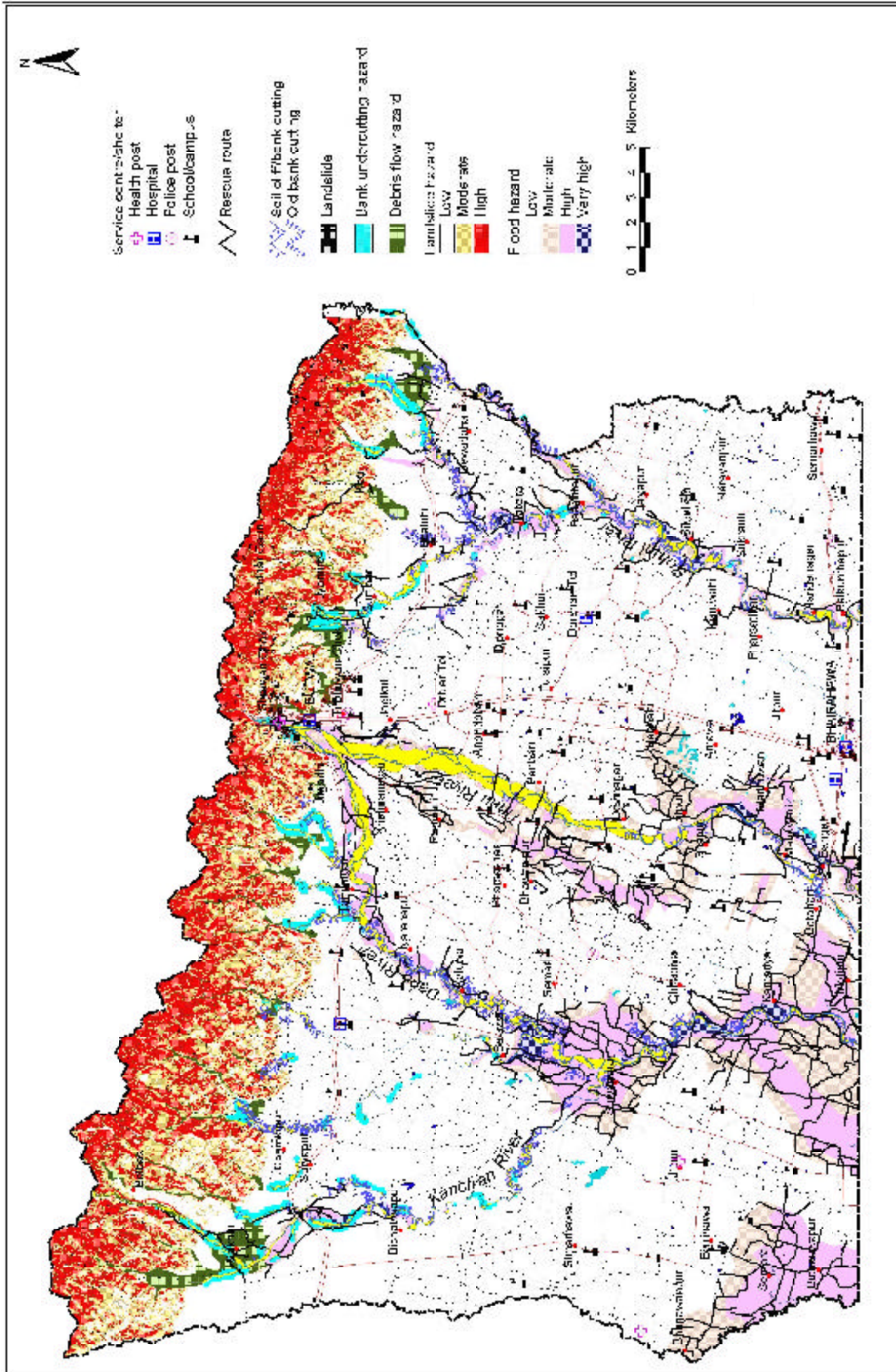


Fig. 11: Integrated hydrological hazard map of the Rupandehi district, west Nepal

Table 8: Distribution of areas under various landslide hazard categories

| Category | Landslide hazard | | Landslide area | |
|--------------|------------------|------------|-----------------|------------|
| | km ² | Per cent | km ² | Per cent |
| Low | 117.42 | 44.28 | 0.15 | 9.83 |
| Moderate | 68.88 | 25.97 | 0.33 | 21.23 |
| High | 78.9 | 29.75 | 1.08 | 68.94 |
| Total | 265.2 | 100 | 1.56 | 100 |

Source: Landslide hazard map

The landslide hazard map was obtained by adding all the above weights (Table 7) and classifying into the following three hazard categories:

- Low (weight less than -1),
- Moderate (between -1 and 0.4), and
- High (more than 0.4).

The distribution of the study area in various hazard categories is shown in Table 8.

Debris flow hazard map

The debris flow hazard map was prepared on the basis of aerial photo and satellite imagery interpretation, field observation, GIS analysis of digital data. For this purpose, the slope gradient ranging between 2 and 20 degrees in the vicinity of gullies and streams was considered. The hazard map was further enhanced applying vertical buffering of bank height measured in the field.

Hydrological hazard map

A unified hydrological hazard map (Fig. 11) of the Rupandehi district was generated by combining all the hazard maps. This map shows landslide, debris flow, and gully erosion hazard in the upper reaches of the Rohini, Tinau, Dano, and Kanchan Rivers as well as flood and bank undercutting hazard in their lower reaches.

RESCUE ROUTES, SERVICE CENTRES, AND SHELTERS

The main rescue routes to nearby service centres and shelters were identified during the field study as well as from the available topographic maps. Nearby schools and university campuses are considered to be the places of shelter whereas hospitals, health posts, and police post are categorised under the service centre.

CONCLUSIONS

The study area has suffered from various types of hydrological disasters, and the prominent ones were landslides, debris flows, floods, bank undercutting, and inundation. Adverse geological conditions, prolonged and high-intensity rainfall, and anthropogenic factors played a

major role in triggering a variety of mass movements in this area. The integrated hydrological hazard mapping methodology was based on a comparison of field data with the computer-generated models. This work showed that it is possible in Nepal to develop a fairly reliable hydrological hazard map based on the available digital data, aerial photographs, and satellite imageries together with a good deal of field observation.

ACKNOWLEDGEMENTS

We acknowledge the Mountain Risk Engineering Unit of Tribhuvan University and the Department of Water-Induced Disaster Prevention, Government of Nepal, for granting permission to publish this paper.

REFERENCES

- Brunsdon, D., Doornkamp, J. C., Fookes, P. G., Jones, D. K. C., and Kelly, J. M. H., 1975, Large-scale geotechnical mapping and highway engineering design. *Quarterly Jour. Engg. Geol.*, v. 8, pp. 227–253.
- Deoja, B, Dhital, M., Thapa, B., and Wagner, A., 1991, *Mountain Risk Engineering Handbook*. ICIMOD, Kathmandu, Nepal, v. 1 and 2, 875 p.
- Dhital, M. R., Upreti, B. N., Dangol, V., Bhandari, A. N., and Bhattarai, T. N., 1991, Engineering geological methods applied in mountain road survey – an example from Baitadi–Darchula Road Study. *Jour Nepal Geol. Soc.*, v. 7, pp. 49–67.
- DoR/USAID, 1986, Rapti Road Assessment Study, Engineering Studies, Final Technical Report (Vol. II). Unpublished report submitted to the Department of Roads (DoR) and the USAID by Luis Berger International Inc. and East Consult (P) Ltd. (unpubl.)
- DPTC (Water Induced Disaster Prevention Technical Centre), 1996, *A Technical Guideline on Landslide Prevention Works*. Government of Nepal, Ministry of Water Resources, Water Induced Disaster Prevention Technical Centre, Pulchowk, Lalitpur, 50 p.
- DPTC, 1993, Flood hazard map of Bagmati River in Tarai. One-page leaflet published by DPTC, Ministry of Water Resources, Pulchowk, Lalitpur.
- HMG Nepal, UNDP, and ICIMOD, 2001, Hazard and Risk Mapping (Electronic copy).
- ILWIS, 1997, *ILWIS 2.1 for Windows, Applications Guide*. Published by ILWIS Department, International Institute for Aerospace Survey and Earth Sciences, Enschede, the Netherlands, 352 p.
- Kojan, E., 1978, Report on landslide problems, Western Hill Road Study, Godavari to Dandeldhura, Nepal. report submitted to USAID (unpubl.).
- Wagner, A., 1981, Rock structure and slope stability study of Waling area, central west Nepal. *Jour. Nepal Geol. Soc.* v. 1(2), pp. 37–43.
- WECS/DHM., 1990, *Methodologies for Estimating Hydrological Characteristics of Ungauged Locations in Nepal* (2 volumes). HMGN Ministry of Water Resources, Water and Energy Commission Secretariat and Department of Hydrology and Meteorology. July 1990.